

## EVALUATION OF THE BEHAVIOUR OF CERAMIC TILES UNDER STATIC LOADING

Dan Mihai CONSTANTINESCU<sup>1</sup>, Marin SANDU<sup>1</sup>, Matei Constantin MIRON<sup>1</sup>,  
Dragos Alexandru APOSTOL<sup>1</sup>, Enikő VOLCEANOV<sup>2</sup>

<sup>1</sup>University “Politehnica” of Bucharest,

<sup>2</sup>Institute for Metallurgical Researches

E-mail: dan.constantinescu@upb.ro

Static testing of zirconium toughened ceramic alumina tiles is done by using the digital image correlation method and applying the loading through a bullet in the middle of the tile. The response of the tile is linear elastic and, in many cases, early and unforeseen failures are obtained due to the geometrical irregularities of the tiles with non-parallel top and bottom surfaces. The displacement and strain fields are monitored till the failure of each tile. The very tough behaviour of the material makes quite challenging the evaluation of the displacements and strain fields; values of strains are very small, in the lower vicinity of the resolution of the ARAMIS system. Experimentally obtained displacements are greater than the ones predicted by theoretical relations and comments on this issue are done. Finite element evaluations of the deflections of the device in which the tile is fixed are also presented. The experimental procedure is reliable and encouraging for the continuation of the research.

*Key words:* Ceramic tiles; Digital image correlation; Finite element method; Failure.

### 1. INTRODUCTION

In general, the strength of ceramics may be comparable to most of the construction steels, accompanied by a brittle behaviour and high capacity of absorbing impact energy, which gives a huge potential for specific applications. Unfortunately, flaws and other defects usually appear during the manufacturing process, and influence the quality of the product. A probabilistic approach in the reliability evaluation based on the Weibull distribution has been accepted in ceramic design [1].

Armour performance has not been successfully correlated to a single material characteristic or static material property due to the dynamic nature of the ballistic event (nano to micro seconds). However, several fundamental material properties have been used to rank various ceramics for the initial evaluation in resisting ballistic impact: chemical composition, microstructure, grain size, density, hardness, elastic modulus, strength, fracture mechanism, fracture toughness. They influence the weight of the armour system, the damage to the projectile, the multi hit resistance, and the energy absorption. The work presented in this paper deals with testing the ceramic tiles used for bullet proof vests and is intended to go further for the ceramics used as add-on armour systems [2]. They can be glued or screwed to the main skull structure and they are easily repairable or upgraded. This is a new protection philosophy, because such a system is produced as a separate kit by a combination of thick ceramic tiles backed by metal or composite plates, designed to achieve different protection levels. Ceramics possess a high protection potential due a moderate density combined to a high compressive strength, but are too brittle to be used without a ductile material backing.

Previous static and low velocity impact tests have been performed experimentally, followed by numerical simulation [3]. The influence of the microstructure of the zirconium toughened alumina ceramics was also analyzed [4]. The chemical composition (grain size, processing, material form, added material components) of alumina ceramics plays an important role and looks to influence their behaviour, strength response, displacement and strain fields.

In this paper a novel experimental technique is used for analyzing the behaviour of the ceramic tiles. A detailed literature survey of the history of photogrammetry and digital image correlation (DIC) systems is

done by Sutton in [5]. In general, DIC is based on the principle of comparing speckle pattern structures on the surface of the deformed and the undeformed specimen or structural component or between any two deformation states. For this purpose, a virtual grid of subsets of a selected size and shape, consisting of certain pixel grey value distributions, is superimposed on the pre-existing or artificially sprayed on surface pattern and followed during deformation by an optical camera system. In this manner, information on the in-plane local strain distribution is gained without assuming a priori the constitutive behaviour of the material. The method finds many applications as in fracture mechanics [6] or fatigue [7] analyses, and its improvements of the sensitivity as discussed in [8] lead to special developments for accurate measurements of the MEMS devices [9].

The digital image correlation (DIC) method proves to be effective in analyzing the response and failure of ceramics and is used in obtaining the results presented hereby. Comments on the analytical displacement solution for the tile and on the numerical simulation results are also done.

## 2. STATIC TESTING PROCEDURE

Initial testing in three-point bending is done by using a 6.3 tf Walter-Bai servo-hydraulic machine with a speed of loading of 0.1 mm/min. Force is applied by a cylinder of 10 mm diameter, and the tile is supported on the same steel cylinders each 5 mm apart from the edge of the tile. Zirconium toughened alumina ceramic tiles of different grades have sizes of about 50 x 50 mm or 40 x 40 mm. The force analogue signal from the testing machine feeds the experimental set-up. Each tile is loaded till failure. One needs to account for standard recommendations for specimens which fulfil the beam theory, but the testing of tiles with the mentioned dimensions was preferred as to obtain more reliable results by having in mind the future impact testing at low and high velocity.

For static tests Höttinger strain gages with one and two measuring grids (gage length of 3 mm) and a MGC Höttinger unit are used to measure strains on the bottom face of the tile (the stretched one), [3]. For the initial tests, two one grid strain gages were positioned in the middle, 5 mm apart from the axis of symmetry, as to measure the longitudinal strain on the direction  $x$ , perpendicular to the line of loading. This was done in order to double the measured signal as we expected small strains due to the tough and fragile behaviour of the ceramic material. Up to a force of about 8,000–10,000 N the response was perfectly linear elastic, and quite soon the specimen broke.

We have to underline that some geometry imperfections were probably the cause for some of the unforeseen events which took place during our tests. Although the supports can rotate in a plane parallel to the line of loading, the top and bottom faces were not always planar; this made possible a non-uniform contact along the support lines and the line of loading and led to unreasonable failures. Such test results were disregarded.

With some more experience and confidence we proceeded with several tests in which our purpose was to establish Poisson's ratio; one of the specimens didn't break at a force close to 11,000 N as all boundary conditions were correctly imposed. A Poisson's ratio of 0.26 resulted. For another test, the curvature of the specimen (non-planar top and bottom faces) gave a loading applied only on the edges of the specimen which slightly increased the transversal strain and diminishes the longitudinal one, and Poisson's ratio became higher, as 0.30. In another test Poisson's ratio came out to be 0.19. We believe that an average value of 0.25 will be appropriate for our material, with a calculated value of the longitudinal modulus of elasticity  $E = 385$  GPa. Again, one should notice that the ceramic material has a very fragile behaviour, and its response is mostly linear elastic up to the final failure.

A more refined testing procedure uses the digital image correlation method and the ARAMIS system [10] as a main experimental setup. The digital image correlation method offers a precise optical solution for deformation measurements. ARAMIS is a non-contact optical deformation measuring system which analyzes, calculates and documents material deformations, being particularly suitable for three-dimensional deformation measurements under static and dynamic loading in order to analyze deformations and strains of real components. If the measuring object has only a few object characteristics, like it is the case with homogeneous surfaces, one needs to prepare such surfaces by applying a stochastic spray pattern. For a 2M system, as the one used in these experiments, the strain measuring range is from 0.01 % up to more than 100 %, and the strain accuracy is up to 0.01 %.

An initial calibration before loading is needed in order to define a zero position; for this type of experiment a caliber of 35×28 mm is used. The chosen facet size is 26×26 with a facet step of 13×13, and thus results a facet field of 87×17 facets. As the deformations are very small the averaging has size 5 and 4 runs are considered.

A second type of tests considers the application of the force directly through a steel bullet in the middle of the ceramic tile, as suggested by the the end user of these results. The speed of loading is of 0.3 mm/min. A specially designed device allows the transmission of the force from vertical to horizontal direction. The opposite face to the one on which the bullet acts can be viewed directly by the cameras of the ARAMIS system. In this way one can notice better what happens on most of the surface of the tile; the tile is supported on its edges along the perimeter. In Fig. 1 can be observed a lateral view of the device fixed in the lower hydraulic grip of the testing machine.



Fig. 1 – Device used for the experimental testing of ceramic tiles by applying the force through a bullet.



Fig. 2 – Lever system to apply the force to the bullet in the middle of the tile.

Figure 2 shows the lever system of the device by which the vertical force from the testing machine is applied to the bullet.

### 3. THEORETICAL SOLUTION

The bending of simply supported rectangular plates leads to a *forced* solution of the differential equations which transforms them into algebraic equations by using double trigonometric series, known as Navier solution [11]. In a  $(x, y)$  coordinate system with the origin in a corner of the plate with edges  $(a \times b)$  and subjected to transverse loading given by a concentrated load  $P$  applied in a point  $(\xi \times \eta)$ , the deflections are obtained from

$$w(x, y) = \frac{P}{\pi^4 abD} \sum_{n=1}^{\infty} \sum_{m=1}^{\infty} \frac{\sin(m\pi\xi/a) \sin(n\pi\eta/b)}{\left[ \left( \frac{m^2}{a^2} \right) + \left( \frac{n^2}{b^2} \right) \right]^2} \sin \frac{m\pi x}{a} \sin \frac{n\pi y}{b}, \quad (1)$$

for  $m, n = 1, 2, 3, \dots$ ;  $D$  is the rigidity of the plate as  $D = Eh^3/12(1-\nu^2)$ , with  $h$  the thickness of the plate and  $E, \nu$  as longitudinal modulus of elasticity (Young's modulus) and Poisson's ratio.

If the concentrated force is applied in the middle ( $\xi = a/2$  and  $\eta = b/2$ ) of a square plate ( $a = b$ ) the *convergence* to the exact solution depends on the number of terms to be chosen as odd  $m$  and  $n$  values (for even  $m$  and  $n$  the function  $\sin$  is zero); by considering eight terms which give a good convergence of the solution, the maximum deflection in the middle of the plate is

$$w_{\max} = 0.0116 \frac{Pa^2}{D} = 0.0116 \frac{12(1-\nu^2)}{Eh^3} Pa^2 = 0.1392(1-\nu^2) \frac{Pa^2}{Eh^3}. \quad (2)$$

Therefore Young's modulus,  $E$ , and Poisson's ratio,  $\nu$ , have an influence on the maximum deflection. In order to analyze this we consider a possible variation of  $\nu$  from 0.17 to 0.41 and values of  $E$  from 385 GPa to 410 GPa with an increment of 5 GPa. The  $E$  values have been chosen as such because we expect for ceramic alumina values of the Young's modulus in between this domain.

The vertical deflection in the centre of the ceramic tile (maximum value) is represented in Fig. 3. The concentrated force is considered as having a generic value of  $P = 10,000$  N. As it depends linearly with the deflection, one can easily calculate from relation (2) the maximum deflection for another given value of the force. In Fig. 3, for  $a = 32$  mm and a thickness of the tile  $h = 10$  mm – as resulting from the experimental setup, the maximum deflection varies over the entire interval of Poisson's ratio variation with 16.7 % for each value of the longitudinal modulus of elasticity (although Poisson's ratio increases 2.4 times). For the same Poisson's ratio, the variation with  $E$  over the considered interval is 7.9 %.

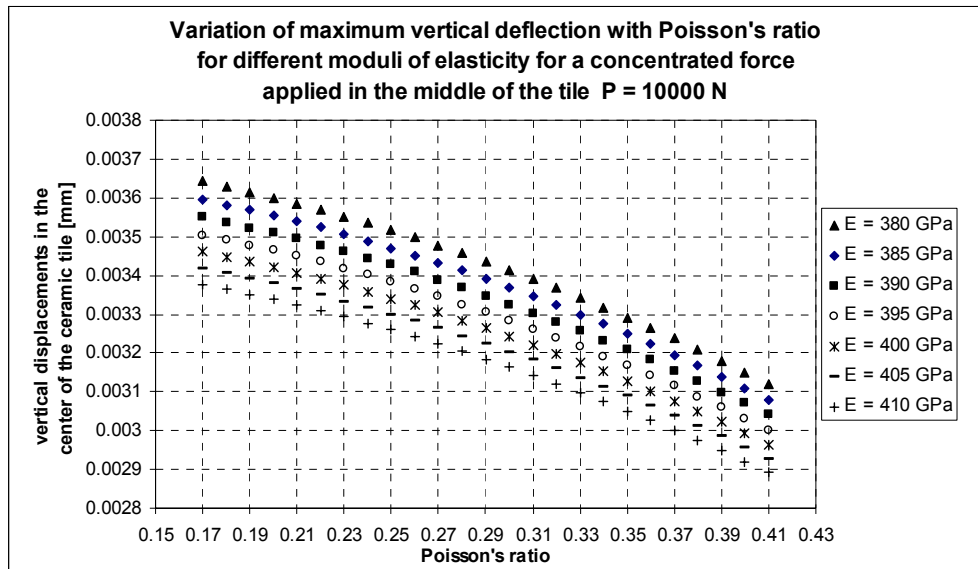


Fig. 3 – Variation of maximum deflection with Poisson's ratio, for different Young's moduli.

#### 4. OBTAINED RESULTS

When applying the force through a bullet, with the ceramic tile in vertical position (fixed in the device as in Figs. 1 and 2) and viewing the tile on the back surface we can analyze the displacements fields on the three directions and the major, minor or equivalent (Mises) strain fields. In this discussion four tiles have been analyzed: two of them are denoted CM 15-1 and CM 15-2 are ceramic zirconium toughened alumina mixed with calcium-magnesium; other two are denoted CMC 15-1 and CMC 15-2, and are mixed with calcium-magnesium-chromium. All tiles are 40×40 mm.

Vertical (out of plane) displacement fields before failure are shown as follows: in Fig. 4 for specimens CM 15-1 and CM 15-2, and in Fig. 5 for specimens CMC 15-1 and CMC 15-2. The surface of the tiles is not perfectly flat; this leads to an uneven support of the tile on the perimeter of the frame of dimensions 32×32 mm. With the exception of tile CM 15-1 which rests more symmetrically on the four corners, the other three tiles are supported more on one or the other of the diagonals of the square. This influences of course the symmetry of the displacement fields and probably the maximum displacement in the middle of the tile. For CM 15-1 the force just before failure is of 11,470 N and the maximum displacement  $w_{\max} = 0.01512$  mm; tiles CM 15-2 and CMC 15-2 fail at much lower forces of 8,103 N, respectively 7,175 N, with maximum deflections in the middle 0.0118 mm and 0.00914 mm.

Table 1 summarizes the main results obtained for the four ceramic tiles. We believe that the results for tile CMC 15-2 can be disregarded due to the non-symmetrical distribution of the displacement and strain fields.

In fact any geometrical imperfections of the ceramic tile will influence the way in which this leans along the edges and will modify the boundary conditions. On the other hand, defects of the material can generate for such a fragile material failures at lower forces than expected.

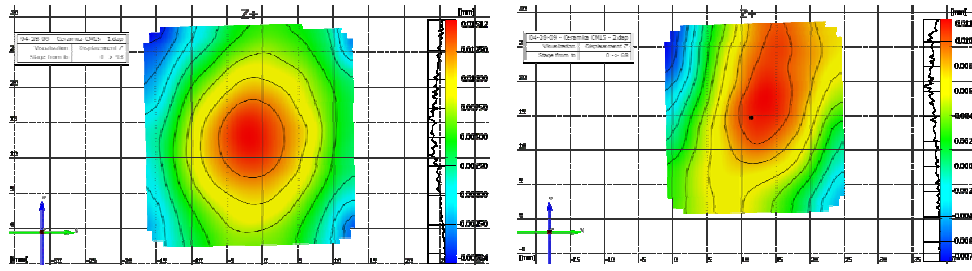


Fig. 4 – Displacement fields before failure for ceramic tiles CM 15-1 and CM 15-2.

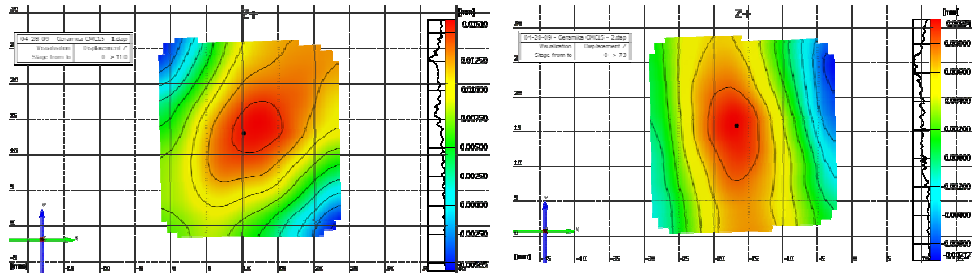


Fig. 5 – Displacement fields before failure for ceramic tiles CMC 15-1 and CMC 15-2.

Major, minor, or Mises strains can be obtained directly by using the software from ARAMIS. The maps of Mises strains are represented in Fig. 6 (for CM 15-1 and CM 15-2) and in Fig. 7 (CMC 15-1 and CMC 15-2).

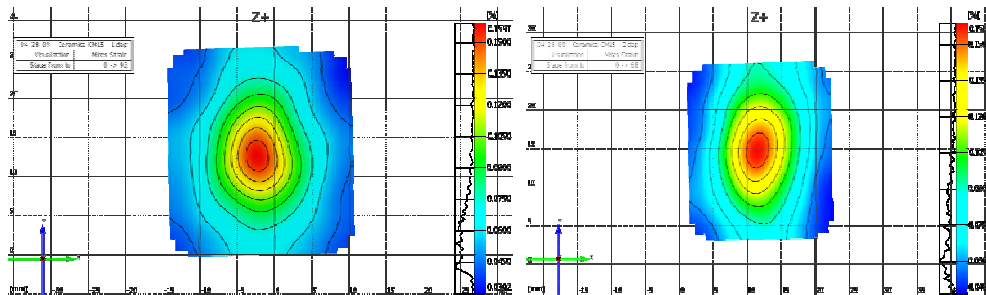


Fig. 6 – Mises strain fields before failure for ceramic tiles CM 15-1 and CM 15-2.

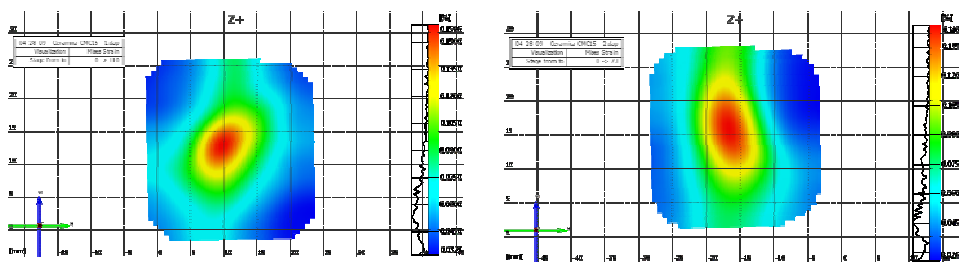


Fig. 7 – Mises strain fields before failure for ceramic tiles CMC 15-1 and CMC 15-2.

Table 1

Obtained displacements and strains by using DIC

Tile	$P_{\max}$ [N]	$w_{\max}$ [mm]	$\epsilon$ major [%]	$\epsilon$ minor [%]	$\epsilon$ Mises [%]
CM 15-1	11470.20	0.01512	0.099	0.0578	0.1591
CM 15-2	8102.62	0.0118	0.115	0.0365	0.1587
CMC 15-1	9493.57	0.0161	0.119	0.0334	0.1596
CMC 15-2	7175.32	0.00914	0.118	0.0176	0.1462

It is to be recognized that the whole device will bend due to the action of the force applied through the bullet to the tile which is supported on the edges to the frame of the device. In Fig. 8 is shown the three-dimensional finite element mesh of the device together with the tile (only half due to symmetry). The frame is less rigid on the top, and horizontal displacements (along the direction of the force) will be greater than on the lower part of the device. On the right side of the figure only one row of elements (towards the frame) of the ceramic tile is represented, and the corresponding displacements are registered.

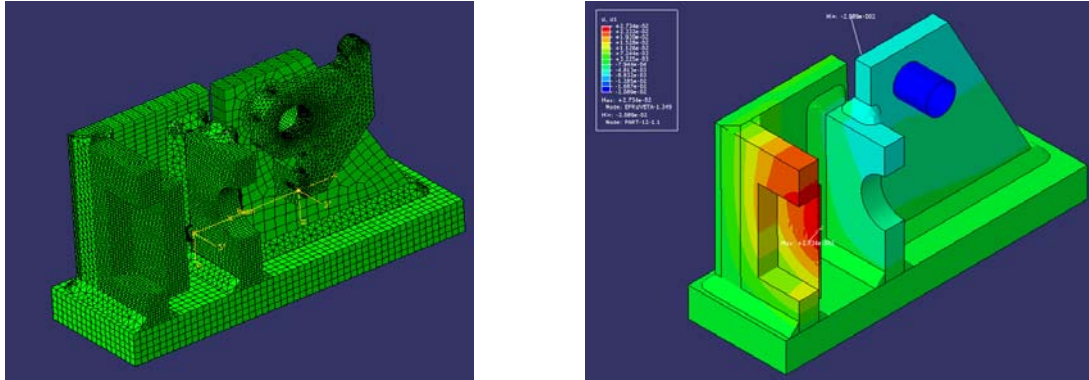


Fig. 8 – Finite element analysis of the deflections of the device under the action of the force applied to the bullet.

The frame of the device is not rigid and in all experimental measurements the displacements due to its elasticity have been subtracted through a command possible in the software of the ARAMIS.

At a force of 10000 N two cases of mechanical properties of the ceramic tile are analyzed: a)  $E = 400$  GPa and  $\nu = 0.3$ ; b)  $E = 385$  GPa and  $\nu = 0.25$ . The total (frame plus tile) horizontal displacements of the tile on its back surface – which is viewed by the ARAMIS system are: a) top 0.0233 mm, bottom 0.0086 mm, left-right along the axis of symmetry of the tile 0.0128; b) top 0.0245 mm, bottom 0.0096 mm, left-right along the axis of symmetry of the tile 0.0132. In the middle of the tile the displacement has the biggest value as about 0.027 mm. It is clear that reducing  $E$  and  $\nu$  the displacements become bigger. These results incorporate the deflections of the frame on which the tile is fixed – a kind of a rigid body motion which may appear and add in the experimental measurements if we don't eliminate it, as in fact we did.

## 5. COMMENTS ON THE RESULTS

The very fragile behaviour of the zirconium toughened alumina material is giving problems in the evaluation of the displacements and strain fields; values of strains are very small, in the lower vicinity of the resolution of the ARAMIS system. More than that, any geometrical imperfection of the tile changes significantly the symmetry of loading, and, of course, the results.

As discussed, the frame of the device on which the tile is supported gives uneven loading and supporting conditions. This is why we use a movement correction algorithm to compensate for the rigid body motion of the tile with respect to the frame on which the tile is leaning. Points along the perimeter of the tile, and very close to the frame, are chosen and included in a best-fit algorithm that transforms all stages of loading to the reference stage, as this perimeter would be fixed. We tested this movement correction by choosing 4 or over 50 points along the perimeter of the tile as to be “fixed”. In the second case resulted a deflection in the middle of the tile with 10 % smaller than in the case with 4 fixed points. The strains are practically the same, as in ARAMIS they are not calculated from displacements but by adjacent facet computations.

In the middle of the tile we expect equal strains on the directions parallel to  $x$  and  $y$  axes, let's say directions  $x'$  and  $y'$ . Only for tiles CM 15-1 and CMC 15-1 we may say that we are close enough to fulfil this condition as: for tile CM 15-1 we obtain  $\varepsilon_{x'} = 0.0994$  % and  $\varepsilon_{y'} = 0.0525$  %, and for tile CMC 15-1 we obtain  $\varepsilon_{x'} = 0.0894$  % and  $\varepsilon_{y'} = 0.0618$  %. So, at the end, the loading of the tile through the device is not symmetric and the state of strain is not biaxial. On the other hand, we obtain strain values towards the minimum strain measuring range.

Experimentally obtained displacements are greater than the ones predicted by theoretical relations. For the maximum values of the displacements in the middle of the tile we get 0.015 mm (CM 15-1), respectively 0.016 mm (CMC 15-1). By using relation (2) with the experimentally obtained values  $E = 385$  GPa and  $\nu = 0.25$  one obtains for the force  $P_{\max} = 11,470$  N (CM 15-1) a theoretical value of the maximum deflection as 0.00398 mm. Which are the reasons for such a difference? Most probably – as already shown – the device by which we apply the force to the bullet deforms and adds a rigid body motion to the displacement of the tile. The movement correction algorithm should compensate this – does it really? Secondly, we measure the deflection on the bottom face of the tile, opposite to the one on which the concentrated force is applied. The theoretical solution gives an average value over the thickness of the tile.

We shouldn't forget that the ceramic tiles have non-parallel top and bottom surfaces which are not even flat. When trying to machine them no improvement was obtained. Even if they became flatter, additional defects were induced and, in all, results didn't improve.

## 6. CONCLUSIONS

Static testing of ceramic alumina tiles is done by using strain gages and digital image correlation. After establishing the elastic constants, the displacement and strain fields are monitored till the failure of each tile. The response of the tile is mainly linear elastic and, in many cases, early failure is obtained due to the geometrical irregularities of the tiles and its non-uniform support over the perimeter. Our present experience emphasizes that the quality of the tile is determinant in obtaining good results.

The digital image correlation method has been used to obtain strains and displacements in the ceramic tiles. Maximum Mises strains are about 0.16 % and maximum deflections in the middle of the tiles about 0.01-0.02 mm. This maximum deflection is almost four times greater than the theoretical one. Several reasons can give an explanation for this difference; probably two are to be retained: the ideal supports of the plate are rigid – which is not our case, and the theoretical deflection is averaged through the thickness of the tile in a more like two-dimensional solution – DIC observation is done on the back surface of the tile, opposite to the one on which we apply the loading through the bullet.

Up to now we haven't found differences in between mixing calcium-magnesium or calcium-magnesium-chromium to the behaviour of the zirconium toughened alumina material. It is true that the number of performed tests has to be increased as the dispersion of results is, unfortunately, important.

The good and encouraging comment is that such an experimental procedure is effective and reliable.

## ACKNOWLEDGEMENTS

This research work is funded by the National Authority for Scientific Research from Romania, contract 81-008/2007.

## REFERENCES

1. ALDINGER, F., BAUMARD, J.F., *Materials: Science and Engineering*, Max-Planck Institut für Metallforschung, Stuttgart, pp. 26–27, 2003.
2. SÁNCHEZ G.V., PARADELA, LAURA SÁNCHEZ, *Analysis of failure of add-on armour for vehicle protection against ballistic impact*, *Engineering Failure Analysis*, **16**, pp. 1837–1845, 2009.
3. CONSTANTINESCU, D.M., SANDU, M., VOLCEANOV, ENIKÖ, GAVAN, M., SOROHAN, ST., *Experimental and numerical analysis of the behaviour of ceramic tiles under impact*, *Key Engineering Materials*, **399**, pp. 161–168, 2009.
4. VOLCEANOV, ENIKÖ, ALDICA, GH. V., VOLCEANOV, A., CONSTANTINESCU, D.M., MOTOC, ŞTEFANIA, *From Conventional to Fast Sintering of Zirconia Toughened Alumina Nanocomposites*, *Mechanical Properties and Performance of Engineering Ceramics and Composites IV*, Eds. D. Singh, W. M. Kriven, **30**, 2, pp. 91–102, Wiley, 2010.
5. SUTTON, M.A., ORTEU, J.-J., SCHREIER, H., *Image Correlation for Shape, Motion and Deformation Measurements; Basic Concepts, Theory and Applications*, Springer, 2009.
6. MEKKY, W., NICHOLSON, P.S., *The fracture toughness of Ni/Al<sub>2</sub>O<sub>3</sub> laminates by digital image correlation I: Experimental crack opening displacement and R-curves*, *Engineering Fracture Mechanics*, **73**, pp. 571–582, 2006.

7. CARROLL, J., EFSTATHIOUS, C., LAMBROS, J., SEHITOGLU, H., HAUBER, B., SPOTTSWOOD, S., CHONA, R., *Investigation of fatigue crack closure using multiscale image correlation experiments*, Engineering Fracture Mechanics, **76**, pp. 2384–2398, 2009.
8. SUTTON, M.A., YAN, J.H., TIWARI, V., SCHREIER, H.W., ORTEU, J.J., *The effect of out-of-plane motion on 2D and 3D digital image correlation measurements*, Optics and Lasers in Engineering, **46**, pp. 746–757, 2008.
9. YA'AKOBOVITZ, A., KRYLOV, S., HANEIN, Y., *Nanoscale displacement measurement of electrostatically actuated micro-devices using optical microscopy and digital image correlation*, Sensors and Actuators A: Physical, **162**, pp. 1–7, 2010.
10. \*\*\* <http://www.gom.com>
11. TIMOSHENKO, S.P., WOINOWSKY-KRIEGER, S., *Teoria plăcilor plane și curbe*, Editura Tehnică, București, 1968.

Received June 28, 2010